

# Implications of the Higgs discovery for the MSSM

Abdelhak Djouadi

*Laboratoire de Physique Théorique, U. Paris-Sud and CNRS, F-91405 Orsay, FRANCE.*

The implications of the discovery of the Higgs boson at the LHC with a mass of approximately 125 GeV are discussed in the context of minimal supersymmetric extension of the Standard Model, the MSSM. Both implications from the Higgs mass and from its production/decay rates are addressed.

## I. INTRODUCTION

The ATLAS and CMS discovery of the particle with a mass of approximately 125 GeV [1] and properties that are compatible with those of a Higgs boson [2] has far reaching consequences for new physics models, in particular, for supersymmetric theories. The latter are widely considered to be very attractive extensions as they naturally protect the Higgs mass against large radiative corrections and stabilise the hierarchy between the electroweak and Planck scales. In the minimal supersymmetric (SUSY) extension, the Minimal Supersymmetric Standard Model (MSSM), two Higgs doublet fields are required to break the electroweak symmetry, leading to five Higgs particles: two CP-even  $h$  and  $H$ , a CP-odd  $A$  and two charged  $H^\pm$  particles [3]. Two parameters are needed to describe the Higgs sector at the tree-level: one Higgs mass, which is generally taken to be that of the pseudoscalar boson  $M_A$ , and the ratio of vacuum expectation values of the two Higgs fields,  $\tan\beta$ , expected to lie in the range  $1 \lesssim \tan\beta \lesssim 60$ . At high  $M_A$  values,  $M_A \gg M_Z$ , one is in the decoupling regime in which the neutral CP-even state  $h$  is light and has almost exactly the properties of the SM Higgs boson, i.e. its couplings to fermions and gauge bosons are the same, while the other CP-even  $H$  and the charged Higgs  $H^\pm$  states are heavy and degenerate in mass with the  $A$  state,  $M_H \approx M_{H^\pm} \approx M_A$ . In this regime, the MSSM Higgs sector thus looks almost exactly as the one of the SM with its unique Higgs boson [2].

There is, however, one major difference between the two cases: while in the SM the Higgs mass is essentially a free parameter (and should simply be smaller than about 1 TeV), the lightest CP-even Higgs particle in the MSSM is bounded from above and, depending on the SUSY parameters that enter the radiative corrections, it is restricted to values  $M_h^{\max} \approx 110\text{--}135$  GeV. Hence, the requirement that the MSSM  $h$  boson coincides with the one observed at the LHC, i.e. with  $M_h \approx 125$  GeV, would place very strong constraints on the MSSM parameters through their contributions to the radiative corrections to the Higgs sector.

Here, we summarise the consequences of such a value of  $M_h$  for the MSSM [4–6]. We first consider the phenomenological MSSM [7] in which the relevant soft SUSY-breaking parameters are allowed to vary freely (but with some restrictions) and constrained MSSM scenarios such as the minimal supergravity (mSUGRA) [8], gauge mediated (GMSB) [9] and anomaly mediated (AMSB) [10] supersymmetry breaking models (for a review, see again Ref. [3]). We also discuss the implications of such an  $M_h$  value for scenarios in which the supersymmetric spectrum is extremely heavy, the so-called split SUSY [11] or high-scale SUSY models [12]. A brief discussion of the Higgs rates and the search for the heavier Higgs states is given.

## II. IMPLICATIONS IN THE PHENOMENOLOGICAL MSSM

In an unconstrained MSSM, there is a large number of soft SUSY-breaking parameters but analyses can be performed in the so-called “phenomenological MSSM” (pMSSM) [7], in which CP conservation, flavour diagonal sfermion mass and coupling matrices and universality of the first and second generations are imposed. The pMSSM involves 22 free parameters in addition to those of the SM: besides  $\tan\beta$  and  $M_A$ , these are the higgsino mass  $\mu$ , the three gaugino masses  $M_{1,2,3}$ , the diagonal left- and right-handed sfermion mass parameters  $m_{\bar{f}_{L,R}}$  and the trilinear sfermion couplings  $A_f$ . Fortunately, besides  $\tan\beta$  and  $M_A$ , only two of them play a major role: the SUSY breaking scale  $M_S = \sqrt{m_{\bar{t}_1} m_{\bar{t}_2}}$  and the mixing parameter in the stop sector,  $X_t = A_t - \mu \cot\beta$ . The maximal value of the  $h$  mass,  $M_h^{\max}$  is given in the leading one-loop approximation by (with some RG improvement using the running top quark mass  $\bar{m}_t$ )

$$M_h \xrightarrow{M_A \gg M_Z} M_Z |\cos 2\beta| + \frac{3\bar{m}_t^4}{2\pi^2 v^2 \sin^2 \beta} \left[ \log \frac{M_S^2}{\bar{m}_t^2} + \frac{X_t^2}{M_S^2} \left( 1 - \frac{X_t^2}{12M_S^2} \right) \right] \quad (1)$$

and is obtained for the following choice of parameters: *i*) a decoupling regime with a heavy  $A$  boson,  $M_A \sim \mathcal{O}(\text{TeV})$ ; *ii*) large values of the parameter  $\tan\beta$ ,  $\tan\beta \gtrsim 10$ ; *iii*) heavy stops, i.e. large  $M_S$  and we choose  $M_S = 3$  TeV as a maximal value; *iv*) a stop trilinear coupling  $X_t = \sqrt{6}M_S$ , the so-called maximal mixing scenario.

An estimate of the upper bound on  $M_h$  can be obtained by adopting the scenario above. To be more precise, we use the program `Suspect` [13] which calculate the Higgs and superparticle spectrum in the MSSM including the most up-to-date information to obtain the maximal value  $M_h^{\max}$ . Following an early analysis [14], we have performed a large scan of the pMSSM 22 parameter space using `Suspect` in an uncorrelated way in the following domains:

$$1 \leq \tan \beta \leq 60, \quad 50 \text{ GeV} \leq M_A \leq 3 \text{ TeV}, \quad -9 \text{ TeV} \leq A_f \leq 9 \text{ TeV}, \\ 50 \text{ GeV} \leq m_{\tilde{f}_L}, m_{\tilde{f}_R}, M_3 \leq 3 \text{ TeV}, \quad 50 \text{ GeV} \leq M_1, M_2, |\mu| \leq 1.5 \text{ TeV}. \quad (2)$$

The results are shown in Fig. 1 where, in the left-hand side, the obtained maximal value  $M_h^{\max}$  is displayed as a function of the ratio of parameters  $X_t/M_S$ . The resulting values are confronted to the mass range  $123 \text{ GeV} \leq M_h \leq 127 \text{ GeV}$  when the parametric uncertainties from the SM inputs and the theoretical uncertainties in the determination of  $M_h$  are included; this uncertainty is obtained by comparing the outputs of `SuSpect` and `FeynHiggs` [15] which use different schemes for the radiative corrections. Hence, only the scenarios with large  $X_t/M_S$  values and, in particular, those close to maximal mixing  $A_t/M_S \approx \sqrt{6}$  survive. The no-mixing scenario  $X_t \approx 0$  is ruled out for  $M_S \lesssim 3 \text{ TeV}$ , while the typical mixing scenario,  $X_t \approx M_S$ , needs large  $M_S$  and moderate to large  $\tan \beta$ . We obtain  $M_h^{\max} = 136, 123$  and  $126 \text{ GeV}$  with maximal, zero and typical mixing.

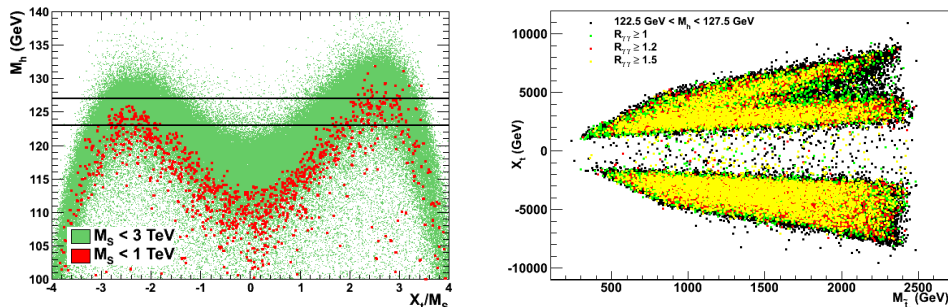


FIG. 1: The maximal value of the  $h$  boson mass as a function of  $X_t/M_S$  in the pMSSM when all other soft SUSY-breaking parameters and  $\tan \beta$  are scanned (left) and the contours for  $123 < M_h < 127 \text{ GeV}$  in the  $[m_{\tilde{t}_1}, X_t]$  plane for some selected range of  $\tan \beta$  values (right). From Ref. [4].

The right-hand side of Fig. 1 shows the contours in the  $[m_{\tilde{t}_1}, X_t]$  plane where we obtain the mass range  $123 \text{ GeV} < M_h < 127 \text{ GeV}$  from our pMSSM scan with  $X_t/M_S \leq 3$ ; the regions in which  $\tan \beta \lesssim 3, 5$  and  $60$  are highlighted. One sees again that a large part of the parameter space is excluded if the Higgs mass constraint is imposed. In particular, large  $m_{\tilde{t}_1}$  values, in general corresponding to large  $M_S$  are favored. However, the possibility that  $m_{\tilde{t}_1}$  is of the order of a few hundred GeV is still allowed, provided that stop mixing (which leads to a significant  $m_{\tilde{t}_1}, m_{\tilde{t}_2}$  splitting) is large. Thus light stops can be still searched for at the LHC...

Squark as well as gluino masses above 1 TeV are also required by the direct searches of SUSY particles at the LHC, confirming the need of high  $M_S$  values to cope with  $M_h \approx 125 \text{ GeV}$ . Nevertheless, relatively light stops and electroweak sparticles such as sleptons, charginos and neutralinos are still possible but the present searches are becoming more and more constraining...

### III. IMPLICATIONS FOR CONSTRAINED MSSM SCENARIOS

In constrained MSSM scenarios (cMSSM), the various soft SUSY-breaking parameters obey a number of universal boundary conditions at a high energy scale, thus reducing the number of basic input parameters to a handful. These inputs are evolved via the MSSM renormalisation group equations down to the low energy scale  $M_S$  where the conditions of proper electroweak symmetry breaking (EWSB) are imposed. Three classes of such models have been widely discussed in the literature: *i*) the minimal supergravity (mSUGRA) model in which SUSY-breaking is assumed to occur in a hidden sector which communicates with the visible sector only via flavour-blind gravitational interactions, leading to universal soft breaking terms ie a common  $m_{1/2}, m_0, A_0$  values for the gaugino, sfermion masses and trilinear couplings, *ii*) the gauge mediated SUSY-breaking (GMSB) model in which SUSY-breaking is communicated to the visible sector via gauge interactions, *iii*) the anomaly mediated SUSY-breaking (AMSB) model in which SUSY-breaking is communicated to the visible sector via a super-Weyl anomaly.

These models are described by  $\tan\beta$ , the sign of  $\mu$  and a few continuous parameters. We adopt the following ranges for the input parameters of these scenarios:

$$\begin{aligned} \text{mSUGRA: } & 50 \text{ GeV} \leq m_0 \leq 3 \text{ TeV}, \quad 50 \text{ GeV} \leq m_{1/2} \leq 3 \text{ TeV}, \quad |A_0| \leq 9 \text{ TeV}; \\ \text{GMSB: } & 10 \text{ TeV} \leq \Lambda \leq 1000 \text{ TeV}, \quad 1 \leq M_{\text{mess}}/\Lambda \leq 10^{11}, \quad N_{\text{mess}} = 1; \\ \text{AMSB: } & 1 \text{ TeV} \leq m_{3/2} \leq 100 \text{ TeV}, \quad 50 \text{ GeV} \leq m_0 \leq 3 \text{ TeV}. \end{aligned}$$

allow for both signs of  $\mu$ , require  $1 \leq \tan\beta \leq 60$  and, to avoid the need for excessive fine-tuning in the EWSB conditions, impose an additional bound  $M_S = M_{\text{EWSB}} = \sqrt{m_{\tilde{t}_1} m_{\tilde{t}_2}} < 3 \text{ TeV}$ . In the case of mSUGRA, one can study special cases such as: no-scale scenario with  $m_0 \approx A_0 \approx 0$ ,  $m_0 \approx 0$  and  $A_0 \approx -\frac{1}{4}m_{1/2}$  which approximately corresponds to the constrained next-to-MSSM (cNMSSM),  $A_0 \approx -m_0$  which corresponds to a very constrained MSSM (VCMSSM), and a non-universal Higgs mass model (NUHM) in which the universal soft SUSY-breaking scalar mass terms are different for the sfermions and for the two Higgs doublet fields.

Using the program `Suspect`, we have performed a full scan of these scenarios. The results for  $M_h^{\text{max}}$  are shown in the left-hand side of Fig. 2 as a function of  $\tan\beta$ , the input parameter that is common to all models, and in the right-hand side of the figure as a function of  $M_S$ .

In contrast to the pMSSM, the various parameters which enter the radiative corrections to the MSSM Higgs sector are not all independent in constrained scenarios as a consequence of the relations between SUSY breaking parameters that are set at the high-energy scale and the requirement that electroweak symmetry breaking is triggered radiatively for each set of input parameters which leads to additional constraints. Hence, it is not possible to freely tune the relevant weak-scale parameters to obtain the maximal value of  $M_h$  given previously. In order to obtain a reliable determination of  $M_h^{\text{max}}$  in a given constrained SUSY scenario, it is necessary to scan through the allowed range of values for all relevant SUSY parameters.

In all cases, the maximal  $M_h$  value is obtained for  $\tan\beta$  around 20. We observe that in the adopted parameter space of the models and with the central values of the SM inputs, the upper  $h$  mass value (rounded to the upper half GeV) is  $M_h^{\text{max}} = 121 \text{ GeV}$  in AMSB, i.e. much less than 125 GeV, while in the GMSB scenario one has  $M_h^{\text{max}} = 121.5 \text{ GeV}$ . Thus, clearly, the two scenarios are disfavoured if the lightest CP-even Higgs particle has indeed a mass in the range  $123 < M_h < 127 \text{ GeV}$ . In the case of mSUGRA, we obtain a maximal value  $M_h^{\text{max}} = 128 \text{ GeV}$  and, thus, some parameter space of the model would still survive the  $M_h$  constraint.

The upper bound on  $M_h$  in these scenarios can be qualitatively understood by considering in each model the allowed values of the trilinear coupling  $A_t$ , which essentially determines the stop mixing parameter  $X_t$  and thus the value of  $M_h$  for a given scale  $M_S$ . In GMSB, one has  $A_t \approx 0$  at relatively low scales and its magnitude does not significantly increase in the evolution down to the scale  $M_S$ ; this implies that we are almost in the no-mixing scenario which gives a low value of  $M_h$  as can be seen from Fig. 1. In AMSB, one has a non-zero  $A_t$  that is fully predicted at any renormalisation scale in terms of the Yukawa and gauge couplings; however, the ratio  $A_t/M_S$  with  $M_S$  determined from the overall SUSY breaking scale  $m_{3/2}$  turns out to be rather small, implying again that we are close to the no-mixing scenario. Finally, in the mSUGRA model, since we have allowed  $A_t$  to vary in a wide range as  $|A_0| \leq 9 \text{ TeV}$ , one can get a large  $A_t/M_S$  ratio which leads to a heavier Higgs particle. However, one cannot easily reach  $A_t$  values such that  $X_t/M_S \approx \sqrt{6}$  so that we are not in the maximal-mixing scenario and the higher upper bound on  $M_h$  in the pMSSM is not reached.

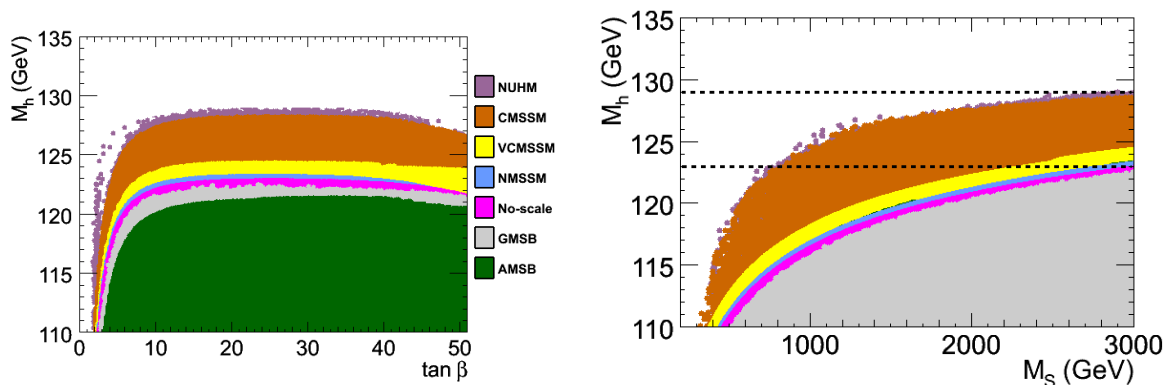


FIG. 2: The maximal value of the  $h$  boson mass as a function of  $\tan\beta$  (left) and  $M_S$  (right) with a scan of all other parameters in various constrained MSSM scenarios. The range  $123 < M_h < 127 \text{ GeV}$  for the light  $h$  boson mass is highlighted. From Ref. [4].

In turn, in two particular cases of mSUGRA that we have discussed in addition, the “no-scale” and the “approximate cNMSSM” scenarios, the upper bound on  $M_h$  is much lower than in the more general mSUGRA

case and, in fact, barely reaches the value  $M_h \approx 123$  GeV. The main reason is that these scenarios involve small values of  $A_0$  at the GUT scale,  $A_0 \approx 0$  for no-scale and  $A_0 \approx -\frac{1}{4}m_{1/2}$  for the cNMSSM. One then obtains  $A_t$  values at the weak scale that are too low to generate a significant stop mixing and, hence, one is again close to the no-mixing scenario. Thus, only a very small fraction of the parameter space of these two sub-classes of the mSUGRA model survive if we impose  $123 < M_h < 127$  GeV. These models hence should have a very heavy spectrum as a value  $M_S \gtrsim 3$  TeV is required to increase  $M_h^{\max}$ . In the VCMSSM,  $M_h \simeq 124.5$  GeV can be reached as  $|A_0|$  can be large for large  $m_0$ ,  $A_0 \approx -m_0$ , allowing at least for typical mixing.

Finally, since the NUHM is more general than mSUGRA as we have two more free parameters, the  $[\tan \beta, M_h]$  area shown in Fig. 2 is larger than in mSUGRA. However, since we are in the decoupling regime and the value of  $M_A$  does not matter much (as long as it is larger than a few hundred GeV) and the key weak-scale parameters entering the determination of  $M_h$ , i.e.  $\tan \beta$ ,  $M_S$  and  $A_t$  are approximately the same in both models, one obtains a bound  $M_h^{\max}$  that is only slightly higher in NUHM compared to mSUGRA. Thus, the same discussion above on mSUGRA, holds also true in the NUHM case.

In the case of these constrained scenarios and in particular in the “general” mSUGRA model, most of the points giving the correct Higgs mass correspond to the decoupling regime of the MSSM Higgs sector and, hence, to an  $h$  boson with SM cross sections and branching ratios. Furthermore, as the resulting SUSY spectrum for  $M_h = 125 \pm 2$  GeV is rather heavy in constrained scenarios, one obtains very small contributions to  $(g-2)_\mu$  and to  $B$ -physics observables such as  $\text{BR}(B_s \rightarrow \mu^+ \mu^-)$ . The correct cosmological density as required by WMAP can be easily implemented. Hence, the resulting spectrum complies with all currently available constraints.

#### IV. SPLIT AND HIGH-SCALE SUSY MODELS

In the preceding discussion, we have always assumed that the SUSY-breaking scale is relatively low,  $M_S \lesssim 3$  TeV, which implies that some of the supersymmetric and heavier Higgs particles could be observed at the LHC or at some other TeV collider. However, as already mentioned, this choice is mainly dictated by fine-tuning considerations which are a rather subjective matter as there is no compelling criterion to quantify the acceptable amount of tuning. One could well have a very large value of  $M_S$  which implies that, except for the lightest  $h$  boson, no other scalar particle is accessible at the LHC or at any foreseen collider.

This argument has been advocated to construct the so-called split SUSY scenario [11] in which the soft SUSY-breaking mass terms for all the scalars of the theory, except for one Higgs doublet, are extremely large, i.e. their common value  $M_S$  is such that  $M_S \gg 1$  TeV (such a situation occurs e.g. in some string motivated models). Instead, the mass parameters for the spin- $\frac{1}{2}$  particles, the gauginos and the higgsinos, are left in the vicinity of the EWSB scale, allowing for a solution to the dark matter problem and a successful gauge coupling unification, the two other SUSY virtues. The split SUSY models are much more predictive than the usual pMSSM as only a handful parameters are needed to describe the low energy theory. Besides the common value  $M_S$  of the soft SUSY-breaking sfermion and one Higgs mass parameters, the basic inputs are essentially the three gaugino masses  $M_1, M_2, M_3$  (which can be unified to a common value at  $M_{\text{GUT}}$  as in mSUGRA), the higgsino parameter  $\mu$  and  $\tan \beta$ . The trilinear couplings  $A_f$ , which are expected to have values close to the EWSB scale, and thus much smaller than  $M_S$ , will in general play a negligible role.

Concerning the Higgs sector, the main feature of split SUSY is that at the high scale  $M_S$ , the boundary condition on the quartic Higgs coupling of the theory is determined by SUSY:

$$\lambda(M_S) = \frac{1}{4} [g^2(M_S) + g'^2(M_S)] \cos^2 2\beta. \quad (3)$$

where  $g$  and  $g'$  are the SU(2) and U(1) gauge couplings. Here,  $\tan \beta$  is not a parameter of the low-energy effective theory: it enters only the boundary condition above and cannot be interpreted as the ratio of two Higgs vacuum expectation values. In this case, it should not be assumed to be larger than unity as usual and will indeed adopt the choice  $1/60 \leq \tan \beta \leq 60$ .

If the scalars are very heavy, they will lead to radiative corrections in the Higgs sector that are significantly enhanced by large logarithms,  $\log(M_{\text{EWSB}}/M_S)$ , where  $M_{\text{EWSB}}$  is the scale set by the gaugino and higgsino masses. In order to have reliable predictions, one has to properly decouple the heavy states from the low-energy theory and resum the large logarithmic corrections; in addition, the radiative corrections due to the gauginos and the higgsinos have to be implemented. Following the early work of Ref. [11], a comprehensive study of the split SUSY spectrum has been performed in Ref. [16]. All the features of the model have been implemented in the Fortran code `SuSpect` [13] upon which the numerical analysis presented in Ref. [4] and summarised here is based.

One can adopt an even more radical attitude than in the split SUSY case and assume that the gauginos and higgsinos are also very heavy, with a mass close to the scale  $M_S$ ; this is the case in the so-called high-scale SUSY model [12]. Here, one abandons not only the SUSY solution to the fine-tuning problem but also the solution to the dark matter problem by means of the LSP and the successful unification of the gauge couplings. However, there will still be a trace of SUSY at low energy: the matching of the SUSY and the low-energy theories is indeed encoded in the Higgs quartic coupling  $\lambda$  given by eq. (3). Hence, even if broken at very high scales, SUSY would still lead to a “light” Higgs whose mass will contain information on  $M_S$  and  $\tan\beta$ .

The treatment of the Higgs sector of the high-scale SUSY scenario is similar to that of split SUSY: one simply needs to decouple the gauginos and higgsinos from the low energy spectrum (in particular remove their contributions to the renormalisation group evolution of the gauge and Yukawa couplings and to the radiative corrections to the  $h$  boson mass) and set their masses to  $M_S$ . We have adapted the version of the program **Suspect** which handles the split SUSY case to also cover the case where  $M_1 \approx M_2 \approx M_3 \approx |\mu| \approx M_S$ . Using this program, we have performed a scan in the  $[\tan\beta, M_S]$  plane to determine the value of  $M_h$  in the split SUSY and high-scale SUSY scenarios. The values given by the PDG for the SM input parameters have been adopted and, in the case of split SUSY, we have chosen  $M_{\text{EWSB}} \approx \sqrt{|M_2\mu|} \approx 246$  GeV for the low scale. The results are shown in Fig. 3. In this figure  $M_h$  is displayed as a function of  $M_S$  for selected values of  $\tan\beta$  in split and high-scale SUSY.

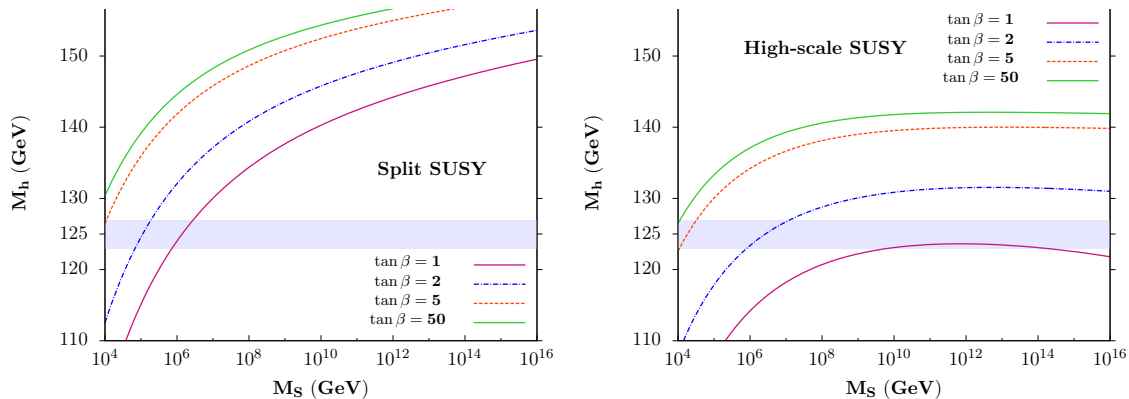


FIG. 3: The value of  $M_h$  as a function of  $M_S$  for several values of  $\tan\beta = 1, 2, 5, 50$  in the split SUSY (left) and high-scale SUSY (right) scenarios. From Ref. [4].

As expected, the maximal  $M_h$  values are obtained at high  $\tan\beta$  and  $M_S$  values and, at the scale  $M_S \approx 10^{16}$  GeV at which the couplings  $g$  and  $g'$  approximately unify in the split SUSY scenario, one obtains  $M_h \approx 160$  GeV for the higher  $\tan\beta = 50$  value. We do not include the error bands in the SM inputs which would lead to an uncertainty of about 2 GeV on  $M_h$ , mainly due to the 1 GeV uncertainty on the top quark mass. In addition, we have assumed the zero-mixing scenario as the parameter  $A_t$  is expected to be much smaller than  $M_S$ ; this approximation might not be valid for  $M_S$  values below 10 TeV and a maximal mixing  $A_t/M_S = \sqrt{6}$  would increase the Higgs mass value by up to 10 GeV at  $M_S = \mathcal{O}(1 \text{ TeV})$  as was discussed earlier for the pMSSM. In the high-scale SUSY scenario, we obtain a value  $M_h \approx 142$  GeV (with again an uncertainty of approximately 2 GeV from the top mass) for high  $\tan\beta$  values and at the unification scale  $M_S \approx 10^{14}$  GeV as in Ref. [12]. Much smaller  $M_h$  values, in the 120 GeV range, can be obtained for lower scales and  $\tan\beta$ .

Hence, the requirement that the Higgs mass is in the range  $123 < M_h < 127$  GeV imposes strong constraints on the parameters of these two models. For this mass range, very large scales are needed for  $\tan\beta \approx 1$  in the split (high-scale) SUSY scenario, while scales not too far from  $M_S \approx 10^4$  GeV are required at high  $\tan\beta$ . Thus, even in these extreme scenarios, SUSY should manifest itself at scales much below  $M_{\text{GUT}}$  if  $M_h \approx 125$  GeV.

## V. IMPLICATIONS FROM THE HIGGS PRODUCTION/DECAY RATES

Note that the  $M_h^{\text{max}}$  values discussed above are obtained with a heavy superparticle spectrum, for which the constraints from flavour physics (such as the limits from the processes  $B_s \rightarrow \mu\mu$  and  $b \rightarrow s\gamma$ ) and sparticle searches (first/second generation squarks and gluinos, but also stops) evaded, and in the decoupling limit in which the  $h$  production cross sections and the decay branching ratios are those of the SM Higgs boson. In the real word, there are other (stringent) constraints on the pMSSM to be included: *i*) the production/decay

rates of the observed Higgs particle, *ii*) the CMS and ATLAS search limits in of the heavier MSSM bosons in the channels  $pp \rightarrow A/H/(h) \rightarrow \tau\tau$  and  $pp \rightarrow t\bar{t}$  with  $t \rightarrow bH^+$ , *iii*) the non observation of heavier Higgses in the  $ZZ, WW, tt$  channels, *iv*) the constraints from sparticle searches and eventually Dark Matter. Some of the constraints provided by the ATLAS and CMS collaborations are shown in Fig. 4.

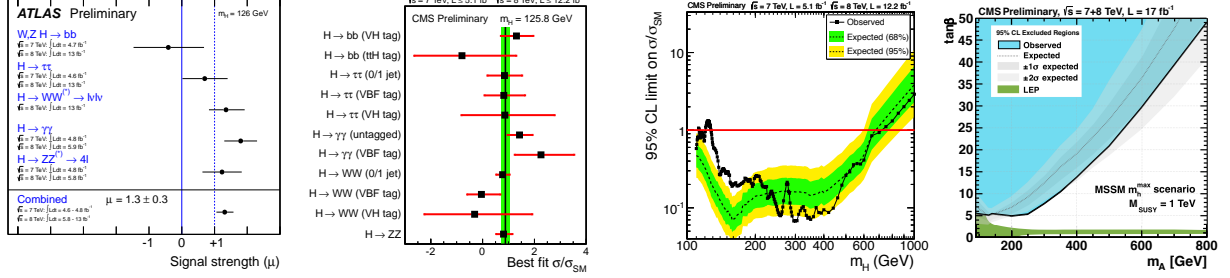


FIG. 4: Constraints from the LHC on the Higgs bosons in the SM and the MSSM. From left to right: the signal strengths in the various Higgs search channels derived by the ATLAS and CMS collaborations with some of the data collected at  $\sqrt{s} = 7+8$  TeV; the 95% confidence level limit provided by CMS on the Higgs cross section normalized to the SM expectation as a function of the Higgs mass with  $\approx 17 \text{ fb}^{-1}$  data collected at  $\sqrt{s} = 7+8$  TeV (this excludes a Higgs boson with a mass below 700 GeV if it has SM couplings and the main channels are  $gg \rightarrow H \rightarrow ZZ, WW$ ); the expected and observed exclusion limits in the  $[\tan\beta, M_A]$  plane in the CMS search of the MSSM neutral Higgs bosons in the channels  $pp \rightarrow h/H/A \rightarrow \tau^+\tau^-$  with  $\approx 17 \text{ fb}^{-1}$  data collected at  $\sqrt{s} = 7+8$  TeV (other processes such as  $pp \rightarrow h/H/A + b\bar{b} \rightarrow 4b$  or charged Higgs production in the channels  $pp \rightarrow t\bar{t}$  with  $t \rightarrow bH^+ \rightarrow b\tau\nu$  lead to less stringent constraints).

An example of output that can be obtained in such a case is given in the left-hand side of Fig. 5 where the parameter space  $[M_A, \tan\beta]$  in a benchmark scenario with  $M_S = 2$  TeV in maximal stop mixing  $X_t = \sqrt{6}M_S$ . The regions excluded by various imposed constraints that we have imposed are indicated. The green area corresponds to the non-observation of Higgs bosons at LEP2 which excludes  $\tan\beta \lesssim 3$  at moderate to large  $M_A$  values. The light blue area is the one ruled out by the CMS results on the search of resonances decaying into  $\tau^+\tau^-$  final states with the 7 TeV data and it touches the LEP2 band at small  $M_A$  but reduces in size when  $M_A$  is increased. The extension of the bound to the 7+8 TeV data with  $\approx 17 \text{ fb}^{-1}$  data is shown by the red line. This constraint is extremely restrictive and for values  $M_A \lesssim 250$  GeV, it excludes almost the entire intermediate and high  $\tan\beta$  regimes,  $\tan\beta \gtrsim 5$ . The constraint is less effective for larger  $M_A$ , but even for  $M_A = 400$  GeV the high  $\tan\beta \gtrsim 10$  region is excluded and one is even sensitive to large values  $M_A \approx 700$  GeV for  $\tan\beta \gtrsim 50$ . Finally, the small visible area in orange is the one excluded by the  $B_s \rightarrow \mu^+\mu^-$  constraint but, in fact, part of the excluded region is hidden by the CMS blue area.

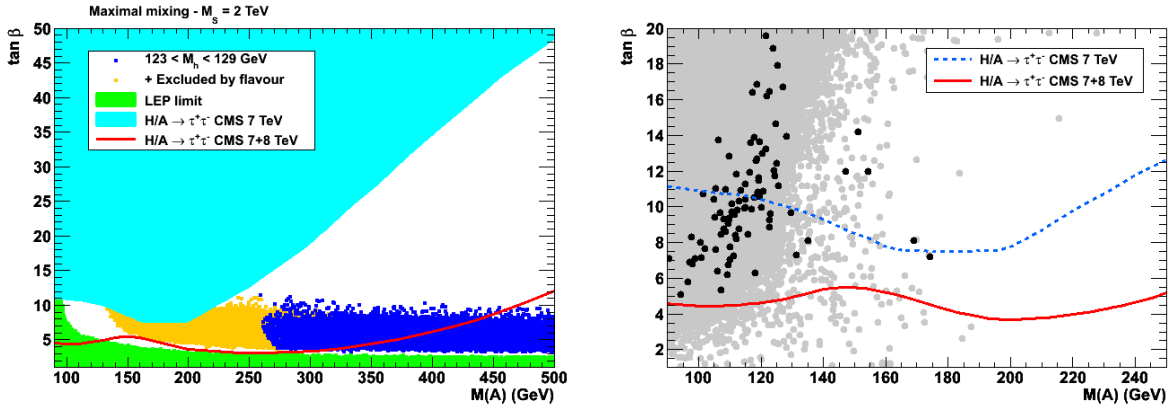


FIG. 5: The maximal value of the  $h$  boson mass as a function of  $X_t/M_S$  in the pMSSM when all other soft SUSY-breaking parameters and  $\tan\beta$  are scanned (left) and the contours for  $123 < M_h < 129$  GeV in the  $[m_{\tilde{t}_1}, X_t]$  plane for some selected range of  $\tan\beta$  values (right). From Ref. [5, 6].

To that, we superimpose the area in which we make the requirement  $123 \leq M_h \leq 129$  GeV, that is indicated in dark blue. This band covers the entire range of  $M_A$  values and leaves only the  $\tan\beta$  values that are comprised between  $\tan\beta \approx 3-5$  and  $\tan\beta \approx 10$ . Between the LEP2 and the “ $M_h$ ” blue band, one has  $M_h < 123$  GeV,

while above the  $M_h$  band, one has  $M_h > 129$  GeV and both areas are excluded. The requirement that the  $h$  boson mass should have the value measured at the LHC, even with the large uncertainty that we assume, provides thus a strong constraint on the  $[M_A, \tan \beta]$  parameter space in the pMSSM.

In addition, we also searched for points in the parameter space in which the boson with mass  $\simeq 125$  GeV is the heavier CP-even  $H$  state which corresponds to values of  $M_A$  of order 100 GeV. Among the  $\approx 10^7$  valid MSSM points of the scan, only  $\approx 1.5 \times 10^{-4}$  correspond to this scenario. However, if we impose that the  $H$  cross sections times branching ratios are compatible with the SM values within a factor of 2 and include the constraints from MSSM Higgs searches in the  $\tau^+\tau^-$  channel, only a few points survive. These are all excluded once flavor constraints are imposed. This is shown in the right-hand of Fig. 5

We note that in Ref. [17] we have considered the production of the heavier  $H, A$  and  $H^\pm$  bosons of the MSSM at the LHC, focusing on the low  $\tan \beta$  regime,  $\tan \beta \lesssim 3-5$ , that is allowed if the SUSY scale is assumed to be very high,  $M_S \gtrsim 10$  TeV. We have first shown that in this case, the requirement that  $M_h \approx 125$  GeV fixes the radiative corrections so that, to a good approximation, one needs only two basic input parameters in the MSSM Higgs sector even at higher orders:  $\tan \beta$  and  $M_A$ . We have then shown that the searches for a heavier SM Higgs boson in the  $WW, ZZ$  final states and the search for new resonances in the  $\tau\tau, t\bar{t}, hZ$  and  $hh$  channels constrain the  $[\tan \beta, M_A]$  parameter space at low  $\tan \beta$  and  $M_A$  values.

The impact of the Higgs decay rates on the parameters of the pMSSM can be estimated by studying the compatibility of the pMSSM points with the results reported by ATLAS and CMS at the LHC and also by the Tevatron experiments. Starting from the scanned set of pMSSM points that are pre-selected for compatibility with the constraints discussed above, we consider the decay channels which allowed the Higgs discovery at the LHC,  $\gamma\gamma$  and  $ZZ$  and include also the  $WW, b\bar{b}$  and  $\tau\tau$  channels. Using the notation  $R_{XX}$  to indicate the Higgs decay branching fraction to the final state  $XX$ ,  $\text{BR}(h \rightarrow XX)$ , normalised to its SM value, we compute the ratios of the product of production cross sections times branching ratios for the pMSSM points to the SM values,  $\mu_{XX}$  for a given  $h \rightarrow XX$  final state,  $\mu_{XX} = \sigma(h) \times \text{BR}(h \rightarrow XX)|_{\text{MSSM/SM}}$ , and compare them to the experimental values with their estimated uncertainties. While most of the results are compatible with the SM expectations within the present accuracy, they highlight a possible enhancement in the observed rates for the  $\gamma\gamma$  channel where ATLAS obtains a  $\approx 2\sigma$  excess if one does not take properly into account the theoretical uncertainties in the production cross section, which are estimated to be significant for the main production channel  $gg \rightarrow h$  [18].

If the excess is not due to a statistical fluctuation (as it appears to be the case since the  $\mu_{\gamma\gamma}$  rate measured by CMS is much closer to the SM value) or to an underestimate of theory uncertainty (which, when properly included, reduces the excess to the  $1\sigma$  level [18]), what are the possible sources for such an enhancement? The answer is given in Fig. 6 where the main possibilities discussed long ago in Refs. [19, 20] have been recently revived in Refs. [21–23] in the light of this possible enhancement.

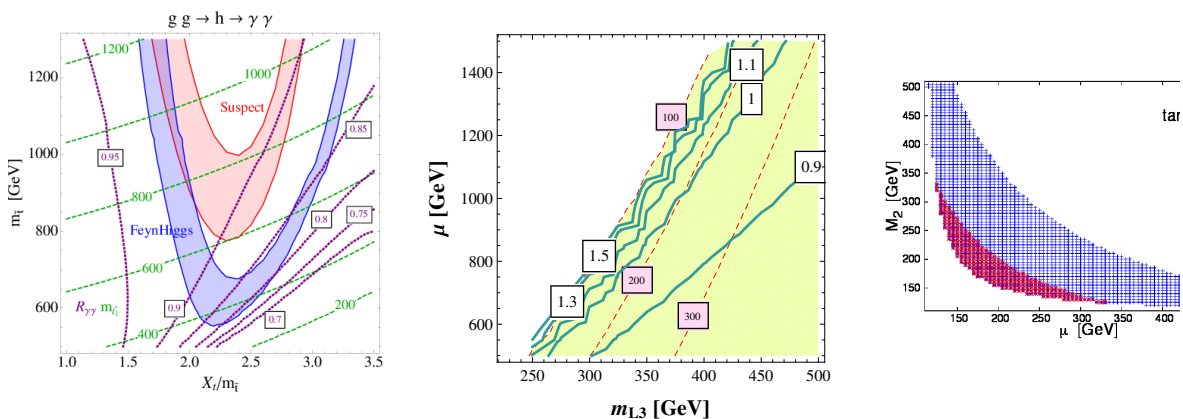


FIG. 6: Possibilities for SUSY particle contributions to the rate  $R_{\gamma\gamma} = \sigma(gg \rightarrow h) \times \text{BR}(h \rightarrow \gamma\gamma)|_{\text{MSSM/SM}}$ . Left: the contours for the rate  $\mu_{\gamma\gamma} \equiv R_{\gamma\gamma}$  in the  $[X_t/m_{\tilde{t}}, m_{\tilde{t}}]$  plane where light stop loops contribute to the  $gg \rightarrow h \rightarrow \gamma\gamma$  rate, provide the ‘correct’  $M_h \approx 125$  GeV when calculated with Suspect or FeynHiggs; however the rate is always smaller than in the SM; from Ref. [21]. Center: contours for  $\mu_{\gamma\gamma}$  in the  $[m_{\tilde{\tau}_L}, \mu]$  plane where light stau’s enhance the  $h \rightarrow \gamma\gamma$  decay at high  $\tan \beta$  values,  $\tan \beta = 60$ ; from Ref. [21]. Right: the rate in the  $[M_2, \mu]$  plane where light charginos enhance  $\mu_{\gamma\gamma}$  by less than 5% (blue) and 10% (red) for  $\tan \beta = 3$ ; from Ref. [23].

Hence, in the MSSM, the enhancement is modest in most cases and is significant only in extreme scenarios.

## VI. CONCLUSIONS

We have discussed the impact of a Standard Model-like Higgs boson with a mass  $M_h \approx 125$  GeV on supersymmetric theories in the context of both unconstrained and constrained MSSM scenarios. We have shown that in the phenomenological MSSM, strong restrictions can be set on the mixing in the top sector and, for instance, the no-mixing scenario is excluded unless the supersymmetry breaking scale is extremely large,  $M_S \gg 1$  TeV, while the maximal mixing scenario is disfavoured for large  $M_S$  and  $\tan\beta$  values.

In constrained MSSM scenarios, the impact is even stronger. Several scenarios, such as minimal AMSB and GMSB are disfavoured as they lead to a too light  $h$  particle. In the mSUGRA case, including the possibility that the Higgs mass parameters are non-universal, the allowed part of the parameter space should have large stop masses and  $A_0$  values. In more constrained versions of this model such as the “no-scale” and approximate “cNMSSM” scenarios, only a very small portion of the parameter space is allowed by the Higgs mass bound.

Finally, significant areas of the parameter space of models with large  $M_S$  values leading to very heavy supersymmetric particles, such as split SUSY or high-scale SUSY, can also be excluded as, in turn, they tend to predict a too heavy Higgs particle with  $M_h \gtrsim 125$  GeV.

## Acknowledgments

I thank the organisers of the conference, in particular Shinya Kanemura and Tetsuo Shindou, for their nice invitation and their patience while waiting for the write-up of my talk. I thank the CERN theory division for the kind hospitality offered to me. This work is supported by the ERC Advanced Grant Higgs@LHC.

- 
- [1] ATLAS collaboration, arXiv:1207.7214 [hep-ex]; CMS collaboration, arXiv:1207.7235 [hep-ex].
  - [2] For a review of the SM Higgs sector, see: A. Djouadi, Phys. Rept. 457 (2008) 1.
  - [3] For a review of the MSSM Higgs sector, see: A. Djouadi, Phys. Rept. 459 (2008) 1.
  - [4] A. Arbey et al., Phys. Lett. B708 (2012) 162.
  - [5] A. Arbey, M. Battaglia, A. Djouadi and F. Mahmoudi, JHEP 1209 (2012) 107.
  - [6] A. Arbey, M. Battaglia, A. Djouadi and F. Mahmoudi, Phys. Lett. B720 (2013) 153.
  - [7] A. Djouadi et al. (MSSM Working Group), hep-ph/9901246.
  - [8] A.H. Chamseddine, R. Arnowitt and P. Nath, Phys. Rev. Lett. 49 (1982) 970; R. Barbieri, S. Ferrara and C. Savoy, Phys. Lett. B119 (1982) 343; L. Hall, J. Lykken and S. Weinberg, Phys. Rev. D27 (1983) 2359; N. Ohta, Prog. Theor. Phys. 70 (1983) 542.
  - [9] M. Dine and W. Fishler, Phys. Lett. B110 (1982) 227; C. Nappi and B. Ovrut, Phys. Lett. B113 (1982) 1785; L. Alvarez-Gaumé, M. Claudson and M. Wise, Nucl. Phys. B207 (1982) 96; M. Dine and A. Nelson, Phys. Rev. D48 (1993) 1277; M. Dine, A. Nelson and Y. Shirman, Phys. Rev. D51 (1995) 1362; G.F. Giudice and R. Rattazzi, Phys. Rept. 322 (1999) 419.
  - [10] L. Randall and R. Sundrum, Nucl. Phys. B557 (1999) 79; G. Giudice, M. Luty, H. Murayama and R. Rattazzi, JHEP 9812 (1998) 027; J. Bagger, T. Moroi and E. Poppitz, JHEP 0004 (2000) 009.
  - [11] N. Arkani-Hamed and S. Dimopoulos, JHEP 0506 (2005) 073; G.F. Giudice and A. Romanino, Nucl. Phys. B699 (2004) 65; J.D. Wells, Phys. Rev. D71 (2005) 015013.
  - [12] See L. Hall and Y. Nomura, JHEP 1003 (2010) 076; G. Giudice and A. Strumia, Nucl.Phys. B858 (2012) 63.
  - [13] A. Djouadi, J.L. Kneur and G. Moultaka, Comput. Phys. Commun. 176 (2007) 426.
  - [14] B. Allanach et al., JHEP 0409 (2004) 044.
  - [15] S. Heinemeyer, W. Hollik and G. Weiglein, Comput. Phys. Commun. 124 (2000) 76.
  - [16] N. Bernal, A. Djouadi and P. Slavich, JHEP 0707 (2007) 016.
  - [17] A. Djouadi and J. Quevillon, arXiv:1304.1787 [hep-ph].
  - [18] J. Baglio, A. Djouadi and R.M. Godbole, Phys.Lett. B716 (2012) 203.
  - [19] A. Djouadi, Phys. Lett. B435 (1998) 101.
  - [20] A. Djouadi, V. Driesen, W. Hollik and J. I. Illana, Eur. Phys. J.C1 (1998) 149.
  - [21] L.J. Hall, D. Pinner and J. Ruderman, JHEP 1204 (2012) 131.
  - [22] M. Carena, S. Gori, N. R. Shah and C. E. M. Wagner, JHEP 1203 (2012) 014.
  - [23] J.A. Casas, J.M. Moreno, K. Rolbieceki and B. Zaldivar, arXiv:1305.3274 [hep-ph].